Shear-Assisted Formation of Cation-Disordered Rocksalt NaMO$_2$ (M = Fe, Mn)

Supplementary Materials

Author List:

Tan Shi[1,2], Penghao Xiao[2], Deok-Hwang Kwon[1], Gopalakrishnan Sai Gautam[2], Khetpakorn Chakarawet[3], Hyunchul Kim[2], Shou-Hang Bo[2, 4]*, Gerbrand Ceder[1,2]*

1. Department of Materials Science and Engineering, University of California, Berkeley, CA 94720, USA

2. Materials Sciences Division, Lawrence Berkeley National Laboratory, Berkeley, CA 94720, USA

3. Department of Chemistry, University of California Berkeley, Berkeley, California 94720, USA

4. University of Michigan – Shanghai Jiao Tong University Joint Institute, Shanghai Jiao Tong University, 800 Dongchuan Road, Minhang District, Shanghai, 200240, P. R. China

* Corresponding authors: shouhang.bo@sjtu.edu.cn; gceder@berkeley.edu

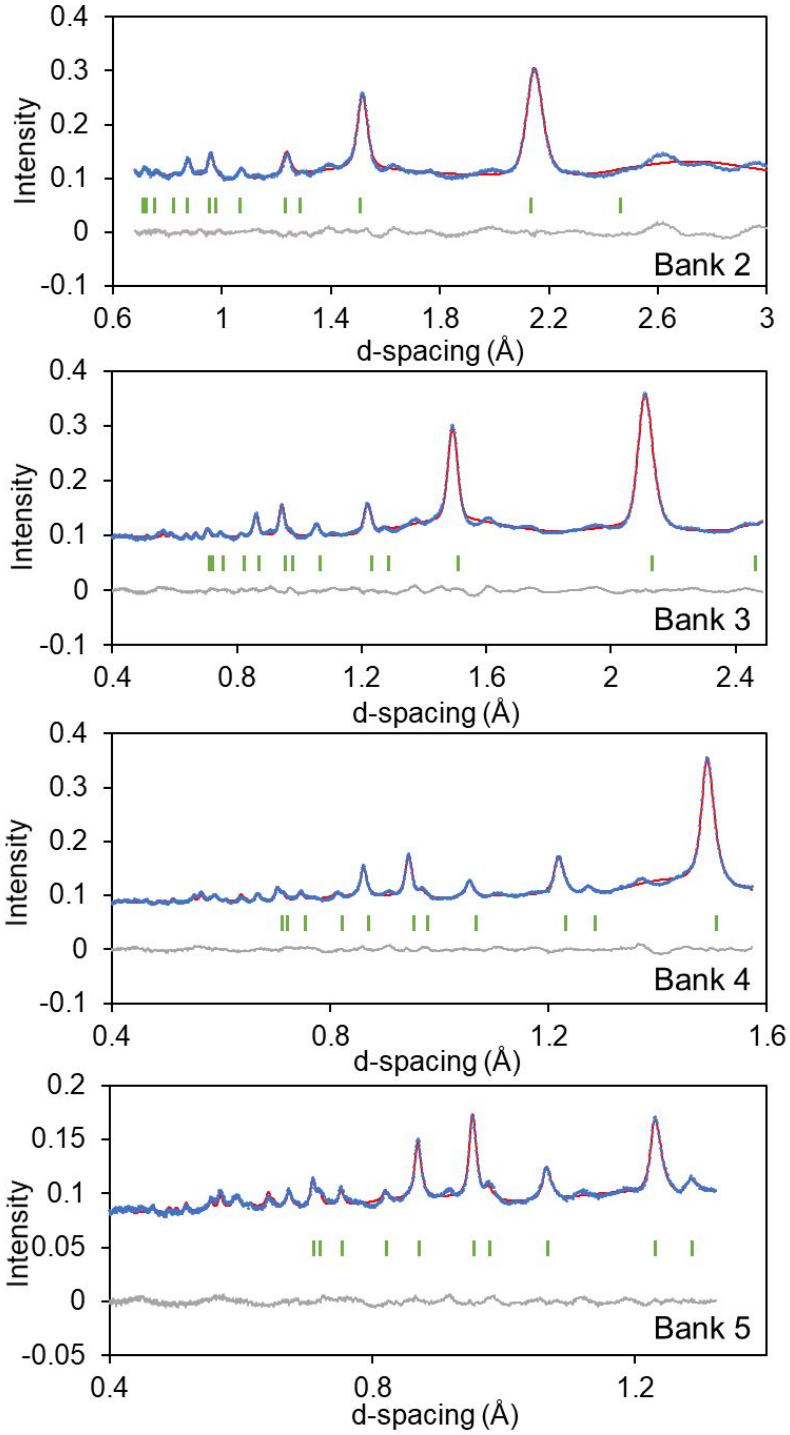

Fig. S1. Neutron diffraction patterns of the as-synthesized rocksalt $NaFeO_2$ fitted to the same structure used in synchrotron diffraction refinement ($Fm3\bar{m}$, a = 4.37 Å). The slight difference in the fitting mainly results from the excess carbon in the sample, which causes additional scattering with neutron.

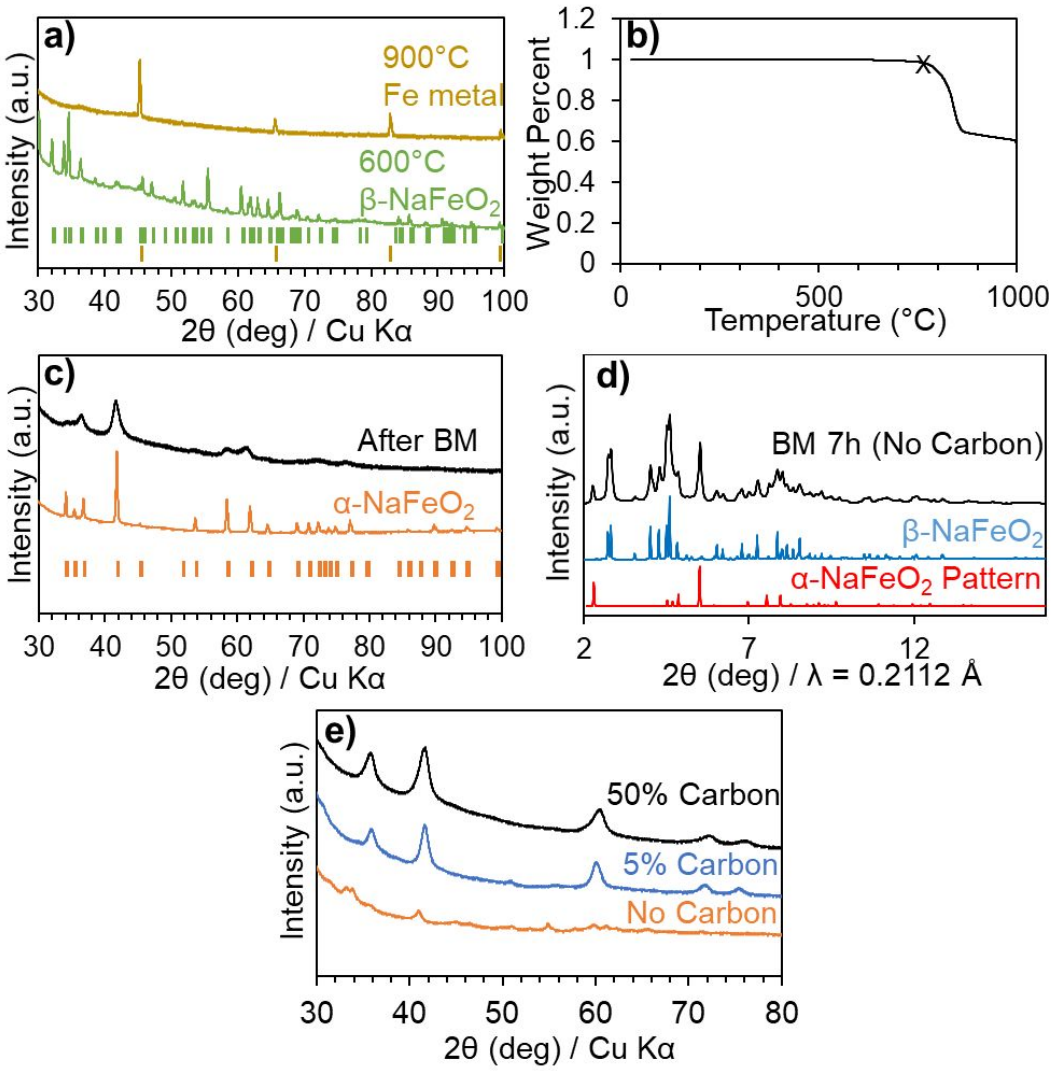

Fig. S2. Cation-disordered rocksalt $NaFeO_2$ cannot be synthesized without ball milling, carbon and β-$NaFeO_2$ as the precursor. a) XRD pattern of the β-$NaFeO_2$ and carbon mixture after heated to different temperatures in Ar atmosphere. After heated to 900°C, the β-$NaFeO_2$ were reduced to Fe metal. **b**) Thermal gravimetric analysis shows the reduction to Fe metal takes place at ~ 750°C. **c**) XRD patterns of the α-$NaFeO_2$ before and after the same ball milling condition as the β-$NaFeO_2$. The only observable change is the peak broadening due to the particle size reduction during the milling process. **d**) XRD pattern of β-$NaFeO_2$ ball milled for 7 hours without carbon shows a majority of the material remains β structure with small amount transformed into α phase. **e)** XRD patterns of the β-$NaFeO_2$ ball milled for 7 hours with different amount of carbon. Rocksalt phase can be observed with as little as 5 wt% carbon added.

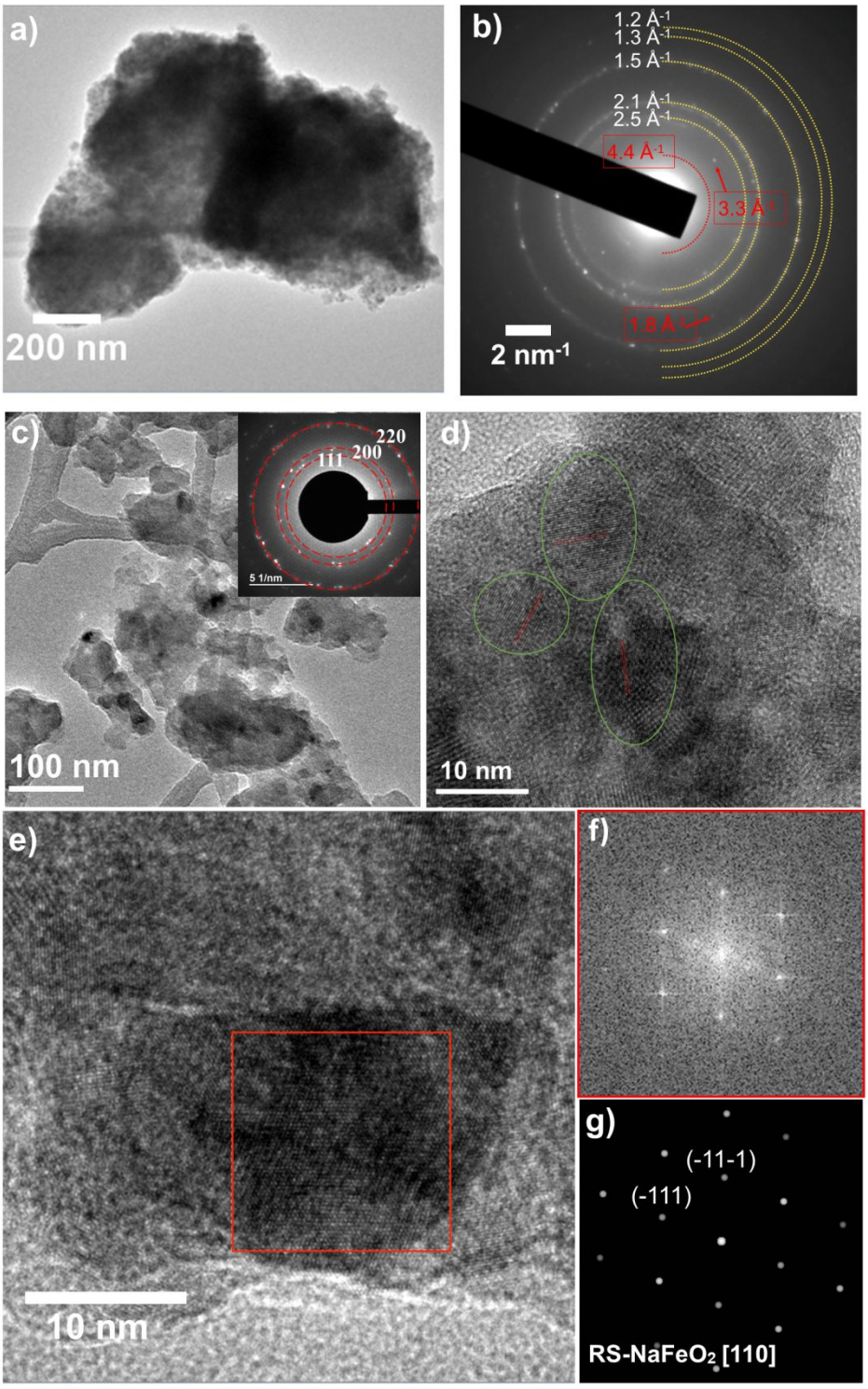

Fig. S3. TEM images and ED patterns of both 3-h-ball-milled (a and b) and 12-h-ball-milled samples (c through g). a) TEM image of a large particle (~ 500 nm) in the 3-h-ball-milled sample. **b)** The electron diffraction of the whole particle shown in **a** showing the coexistence of rocksalt

phase and β-$NaFeO_2$ phase. The majority diffraction signal can be identified as disordered rocksalt (labelled yellow). However, β-$NaFeO_2$ diffraction spots are also visible (labelled red). **c)** TEM image and electron diffraction pattern (insert) of 12-h-ball-milled sample. The small dark spots are the nano-sized $NaFeO_2$ particles embedded in carbon matrix, which is shown as the light and cloudy area. The electron diffraction pattern also shows a rocksalt structure symmetry, consistent with the X-ray diffraction data. **d)** High magnification TEM image showing the grain sizes of 12-h-ball-milled sample has been reduced to < 10 nm. Several grains are highlighted by the green circles and their respective lattice fringes are indicated by the red dash lines. **e)** High magnification TEM image of a single grain in $NaFeO_2$ particle in the12-h-ball-milled sample. **f)** FFT of the area in the red square in **e**. **g)** Simulated diffraction spots of an ideal disordered rocksalt $NaFeO_2$ structure showing good agreement with **f**.

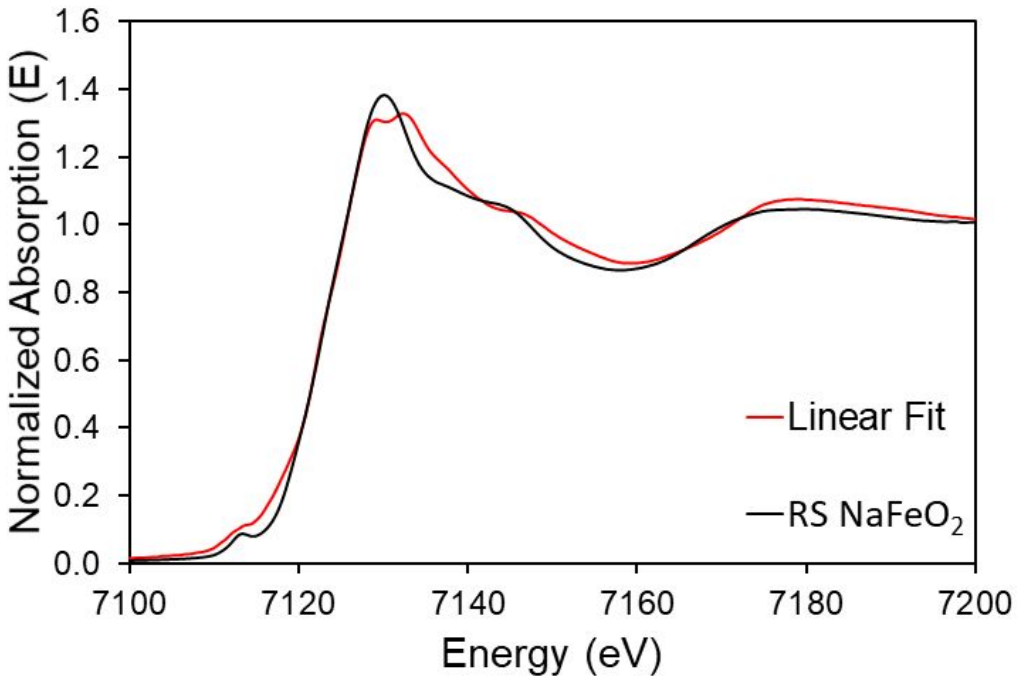

Fig. S4. XANES spectra of as synthesized $NaFeO_2$ fitted using linear combination method with 32.2% FeO and 67.8% Fe_2O_3.

-

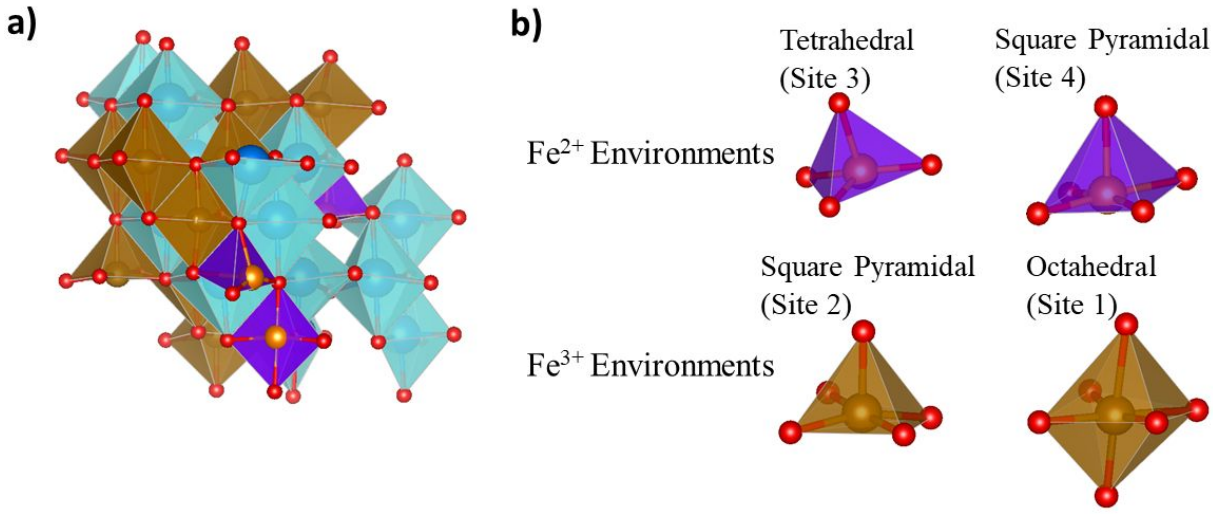

Fig. S5. a) DFT calculated structure for cation disordered rocksalt $NaFeO_2$ with 6% O vacancies. Maximum Fe-O bond was set to 4.5 Å. **b)** Four different Fe local environments isolated from DFT calculation structure from a). There are two different environments for Fe^{2+} (resembling tetrahedral and square pyramidal coordination) and two for Fe^{3+} (resembling octahedral and square pyramidal coordination). This coordination difference rises from their different valence states and their relative positions with respect to the O vacancies. It is expected that oxygen vacancies are more likely to be created near a reduced Fe ion (Fe^{2+}), and therefore resulting in a lower averaged coordination number for Fe^{2+} ions compared to Fe^{3+} ions. All sites show large distortions; therefore, their chemical shifts (δ) and quadruple splittings (ΔEQ) cannot be directly compared with reference values. Instead, each fitting profile is assigned to the site that has closest reference values for both δ and ΔEQ.

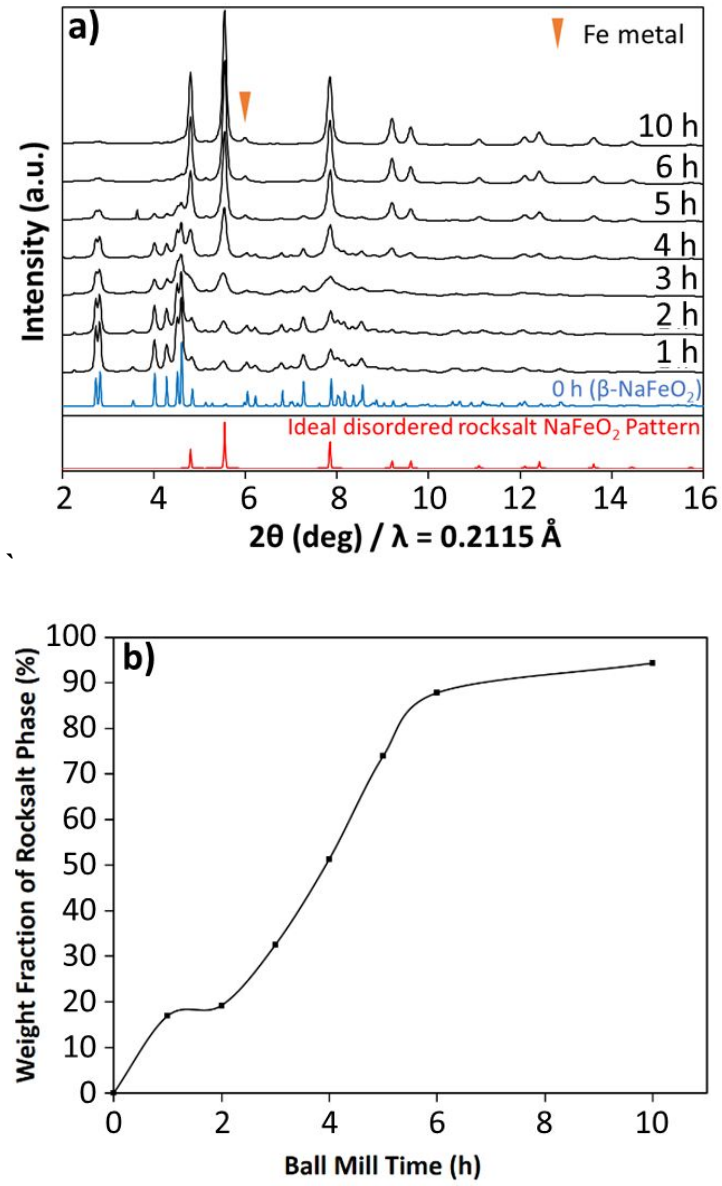

Fig. S6. a) Synchrotron XRD patterns of β-$NaFeO_2$ after different ball milling times. **b)** Estimated weight fraction of rocksalt phase during ball milling obtained from Rietveld refinement of synchrotron XRD data.

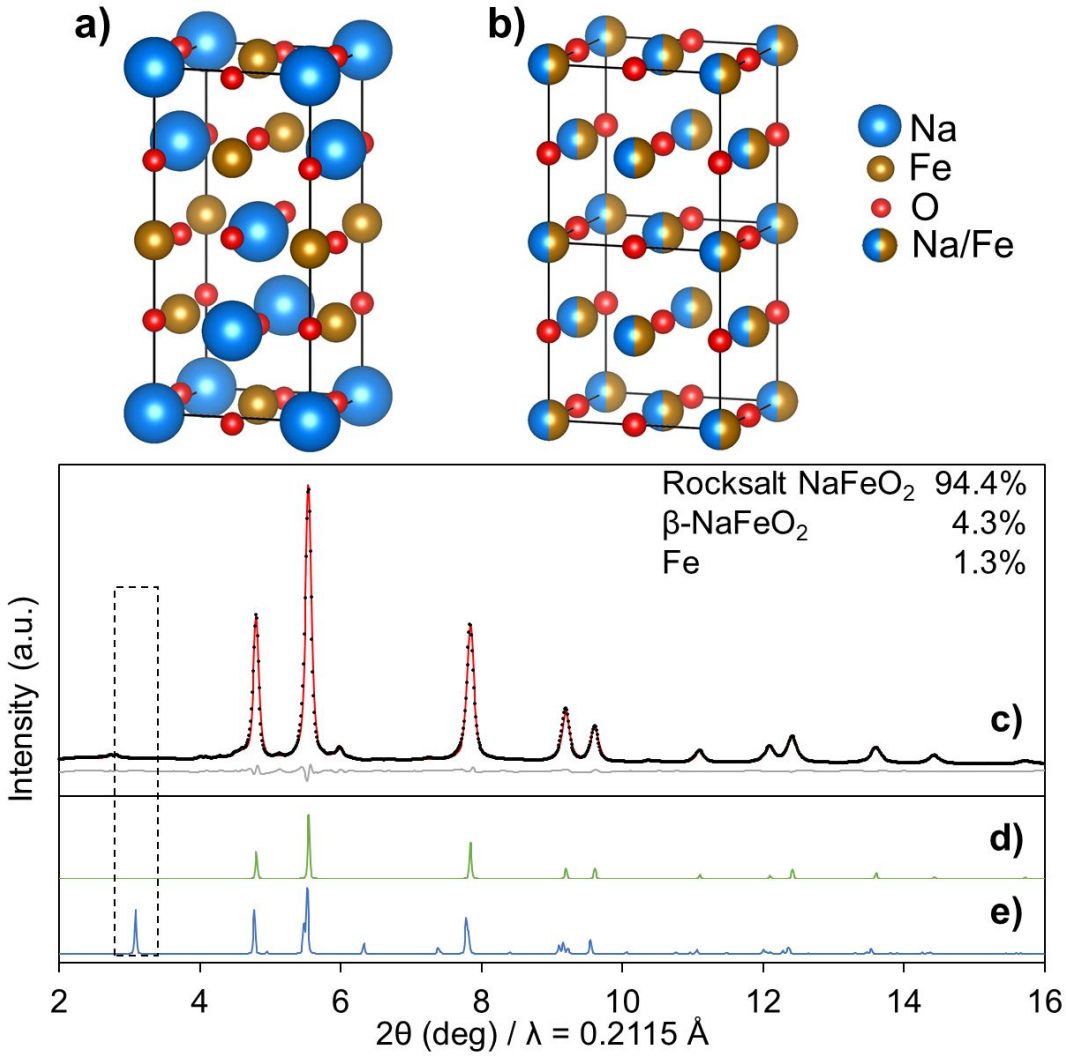

Fig. S7. a) Structure model of ordered rocksalt $NaFeO_2$ with zigzag cation ordering inherited from β-$NaFeO_2$ (similar to γ-$LiFeO_2$ ordering). **b)** Structure model of cation disordered rocksalt $NaFeO_2$ with Na and Fe atom sharing the same site. **c)** Rietveld-refined synchrotron X-ray diffraction pattern of as prepared cation-disordered rocksalt $NaFeO_2$ with small amount of Fe impurity and residual β-$NaFeO_2$. Note that the cation ordering peak at ~ 3 Å is absent. **d)** Simulated diffraction pattern of ideal disordered rocksalt $NaFeO_2$ shown in b). **e)** Simulated diffraction pattern of ordered rocksalt $NaFeO_2$ with zigzag cation ordering inherited from β-$NaFeO_2$ (shown in a)).

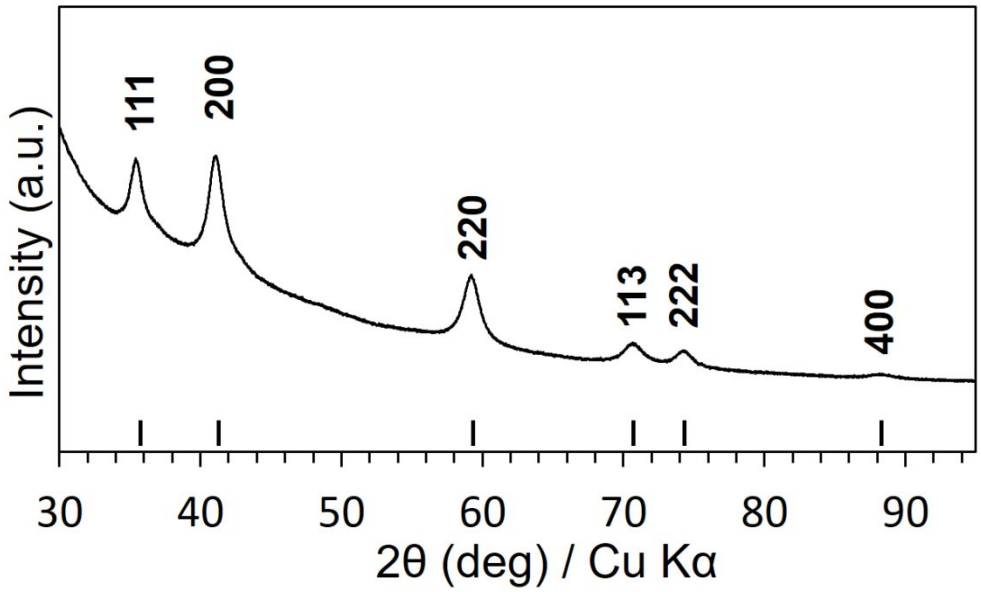

Fig. S8. XRD pattern of disordered rocksalt $NaMnO_2$ synthesized by ball milling β-$NaMnO_2$ with carbon. The sloping background is due to the Kapton tape used to prevent air exposure during the XRD scan.

Phase name	**Cation-Disordered Rocksalt $NaFeO_2$**					
Atom	**Site**	**occupancy**	**x**	**y**	**z**	**U**
Na	4a	0.5	0	0	0	0.005982
Fe	4a	0.5	0	0	0	0.005986
O	4b	0.95	0	0	0.5	0.03337

Space group: $Fm\bar{3}m$; a = 4.37 Å; R_w = 2.82; goodness of fit = 2.74.

Table S1. Synchrotron XRD data Rietveld refinement results for cation-disordered rocksalt $NaFeO_2$.

$NaFeO_2$ Structure	O Vacancy (eV)	2 O vacancies (eV)
β	3.4	6.7
Rocksalt	2.8	5.6
α (ground state)	2.9	6.8

Table S2. DFT calculated defect formation energies for different $NaFeO_2$ structures. Rocksalt structure shows the lowest formation energy for oxygen vacancies among the three, and the energy differences become greater as the vacancy concentration increases. Oxygen vacancy formation energies are determined by removing Oxygen from a supercell with 32 oxygen atoms. Different vacancy positions are tested to find the lowest energy configuration.

O vacancy conc.	0	3.1	6.3
E_{RS}-E_{β} (meV/atom)	50.25	37.6	22.9

Table S3. DFT calculations showing decreasing energy differences between rocksalt structure and β structure $NaFeO_2$ with increasing oxygen vacancy concentration.

Bond	ΔE (eV)	N	R (Å)	DWF (10^{-3} Å^2)	R-factor (%)
Fe-O1	-0.41 ± 2.01	3	1.96 ± 0.02	7.06 ± 4.01	0.94
Fe-O2		2	2.10 ± 0.04	7.06 ± 4.01	
Fe-O3		1	2.63 ± 0.11	7.06 ± 4.01	
Fe-Na1		3	2.88 ± 0.05	9.05 ± 10.01	
Fe-Fe1		6	3.09 ± 0.04	10.24 ± 1.77	
Fe-Na2		3	3.32 ± 0.07	9.05 ± 10.01	

ΔE: inner shell potential shift; N: coordination numbers; R: bond distance; DWF: Debye–Waller factor (σ^2, disorder).

Table S4. Curve fitting results for the Fe K-edge EXAFS spectrum of the as-prepared cation-disordered rocksalt $NaFeO_2$ shown in Fig. 2b.

Empirical Pair Potential

The empirical pair potential is of the following form with parameters listed in Table S4:

$$V_{ij} = \frac{q_i q_j}{r_{ij}} + 4\varepsilon_{ij}\{(\frac{\sigma_{ij}}{r_{ij}})^{12} - (\frac{\sigma_{ij}}{r_{ij}})^{6}\}$$

	q **(e)**	***ε*****(eV)**	***σ*****(Å)**
Na	0.525671	8.65971E-04	1.18606
Fe	1.455048	2.27328E-05	1.58667
O	-0.990359	1.78159E-06	6.31161

Table S5. Parameters for the $NaFeO_2$ pair potential.

For the Lennard-Jones part, combination rules are used when calculating interactions between different species. The pair potential well reproduces relative stabilities between the α-, β- and ordered rocksalt $NaFeO_2$ from DFT. Fig. S9 shows the minimum energy path calculated by the pair potential comparing with the DFT one (Fig. 6a, black curve).

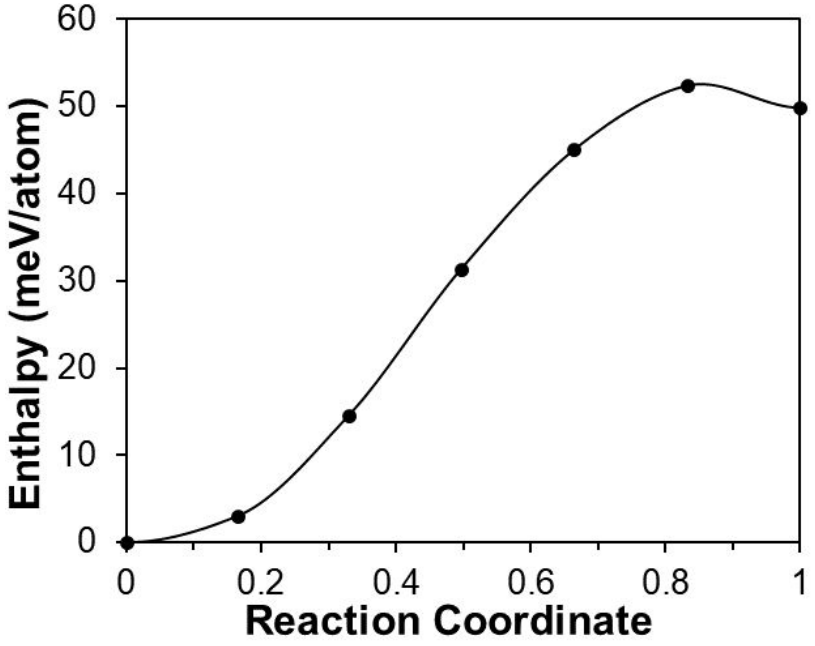

Fig. S9. The minimum energy path for β to rocksalt $NaFeO_2$ phase transition calculated with the empirical pair potential.